Growth of tactoidal droplets during the first-order isotropic to nematic phase transition of F-actin

Patrick W. Oakes, Jorge Viamontes, and Jay X. Tang*
Department of Physics, Brown University, Providence, Rhode Island 02912, USA
(Received 14 December 2006; revised manuscript received 20 March 2007; published 1 June 2007)

We report on the observed characteristics of the first-order phase transition of F-actin from the isotropic state to the nematic liquid-crystalline state. Solutions of short average filament length F-actin at appropriate concentrations phase separate to form tactoidal droplets. These tactoids are the result of the minimization of their free energy and show a bipolar director field connecting two opposite poles. The tactoids are shown to form through two distinct mechanisms: nucleation and growth and spinodal decomposition. Both mechanisms produce tactoids with final domain sizes that are of the same order of magnitude. Additionally, analysis of the system shows several features of metastability. The solution can exist in a variety of steady states near equilibrium and can be easily perturbed, settling in one prescribed by the path followed in phase space.

DOI: 10.1103/PhysRevE.75.061902 PACS number(s): 87.16.Ka, 87.15.Nn, 64.70.Md

I. INTRODUCTION

The cytoskeleton, a viscoelastic mesh of protein filaments, plays essential roles in many cellular functions such as shape regulation, motility, and signal transduction across the cell periphery [1]. A ubiquitous protein in the cytoskeleton, actin is pivotal to the successful execution of these functions. Actin is found both as globular monomers (G-actin) and as filaments (F-actin) and is constantly interchanging between these two dynamic states. The filaments form through the polymerization of the monomers, a process facilitated by a number of accessory proteins found in cells. These filaments are helical in nature with a diameter of approximately 8 nm [2], and it is their extension which is responsible for a number of motility events [3].

The process of polymerization and depolymerization in actin has been extensively studied [4]. In the presence of adenosine triphosphate (ATP), polymerization is not reversible. Each filament consists of a barbed end, where monomers are added, and a pointed end, where monomers are disassociated from the filament. This results in a steady-state process termed treadmilling, where the net addition of monomers to the barbed end is equally matched by a net dissociation from the pointed end [5,6]. This constant cycling is a key factor in the function of cell motility. Furthermore, solutions of F-actin are polydisperse, showing a range of filament lengths [7,8].

The persistence length of F-actin has been measured to be $15-18\ \mu$m [9,10]. This is larger than the average filament length typically found both in cells and *in vitro*. As a result, actin filaments are modeled as semiflexible rods. There have been a number of different studies regarding the remarkable properties of F-actin. For instance, extensive research has been undertaken to explore the viscoelastic properties of F-actin networks [11–13], their phase transitions [14–16], and also the ability of F-actin to form bundles in the presence of polycationic agents [17] or actin binding proteins [18–20].

The phase transition undergone by F-actin filaments sets the theme of this work. A solution of F-actin is found to form a nematic liquid-crystalline phase at high protein concentrations, on the order of mg/ml, consistent with the semiflexible rod model. F-actin is expected to behave like solutions of other rodlike macromolecules, which are known to undergo a clear first-order phase transition between isotropic and nematic states [21]. Indeed, the onset concentration of this transition has been shown to be inversely proportional to the average filament length ℓ of the F-actin in the solution [14–16,22]. This agrees well with the statistical mechanical theories that have been put forth [23–26].

Solutions of F-actin can easily be found in both isotropic and nematic states. Optical birefringence measurements show that the filaments are clearly aligned at high concentrations and in the nematic state. As expected, no birefringence is seen at low concentrations as the solution is in the isotropic state. Under the right conditions alternating high- and low-retardance regions have been observed, especially near the walls of capillary tubes and air-liquid interfaces [15,16,22,27]. These striped birefringence patterns have been attributed to a spontaneous separation of the solution into isotropic and nematic regions [22]. A first-order transition is expected to be discontinuous, but recent experimental results [15,16] suggest that the isotropic to nematic transition in F-actin is continuous in both alignment and concentration. Interestingly, we have just recently shown that for $\ell < 2\ \mu$m a true first-order phase separation does indeed occur [28]. This phase separation results in the familiar tactoid shape, first reported by Zocher in 1925 in a vanadium pentoxide system [29]. The term tactoid was coined a few years later [30] and has since been used to describe such shapes in many systems [31,32].

For solutions with $\ell \geq 2\ \mu$m, the transition is no longer marked with clear phase separation. Instead, there exists a defined range of concentrations over which the orientational order parameter grows from zero to a saturation value [7]. We have postulated that the long length and flexibility of the filaments ultimately entangles the network and results in a continuous transition from the isotropic to the nematic phase [16,28]. It is also possible that the solution could be undergoing gelation, hindering the phase separation. In our previous reports on this subject we suggested that this result might

*Correspondence address: Jay_Tang@Brown.edu

 ©2007 The American Physical Society

be pertinent to the findings of Lammert, Rokhsar, and Toner [33,34]. Direct experimental evidence for any of these predictions is lacking however, calling attention to the need for further studies.

Our aim in this paper is to characterize in detail the isotropic to nematic transition of F-actin, primarily under the conditions where a first-order isotropic to nematic phase separation occurs. Using both polarization microscopy and optical birefringence measurements, the distinctive tactoid shape is analyzed and found to be consistent with the theoretical and numerical treatments derived from the minimization of the free energy of a liquid crystal [35–39]. In addition to studying the equilibrium phase separation that occurs, we have analyzed the growth of the tactoids and will show that F-actin in solution can undergo the process of nucleation and growth and spinodal decomposition during phase separation. Finally, many aspects of our results suggest that the solution often is not in true equilibrium, but rather settles in a metastable state. We will explore this issue through the course of this work and discuss its implications.

II. MATERIALS AND METHODS

A. Sample preparation

Actin was extracted from rabbit skeletal muscle following the technique of Pardee and Spudich [40]. The extracted actin, typically concentrated to over 10 mg/ml, was frozen with liquid nitrogen and stored at −80 °C. For experiments, the actin was thawed rapidly in a heatblock to 25 °C and centrifuged for 5 min at ~7000 g. The G-actin was polymerized by addition of the salts KCl and $MgCl_2$ to concentrations of 50 mM and 2 mM, respectively. An end-capping and filament-severing protein, gelsolin, was added to regulate the average filament length ℓ of the actin filaments [17,41]. The average filament length was estimated using the ratio of gelsolin to actin [41] and confirmed through measurements of selected samples [16]. The phase separation of F-actin is a function of both the average filament length and the solution concentration. In our experiments we found it more practical to probe the full scope of the transition region by altering the average filament length instead of varying the concentration. When dilutions were necessary they were performed from the concentrated stock solution prior to the actin being polymerized to avoid problems in pipetting caused by a drastic increase in the viscosity of polymerized solutions.

Solutions of polymerized actin were injected into rectangular capillary tubes (VitroCom Inc., Mt. Lakes, NJ) with cross-sectional dimensions of 0.2×2 mm^2. Each capillary was immediately sealed with an inert glue to eliminate flow and evaporation from the system. To ensure that the results were independent of the injection method used for sample preparation, additional samples were prepared by placing drops of solution between a slide and a coverslip. Tactoids were reproducibility observed in this alternative method of sample preparation as well.

B. Fluorescence labeling and imaging

The actin filaments were labeled with tetramethylrhodamine isothiocyanate (TRITC) conjugated phalloidin (Sigma, St. Louis, MO). Phalloidin, a tiny molecule compared to actin, binds tightly to filamentous actin and stabilizes the filament [42]. The phalloidin molecule binds randomly along the side of the actin filament but does not bind to individual monomers. Due to the statistically large number of molecules and the randomness of the binding events, the fluorescence intensity can be used to quantitatively determine differences in concentration between domains in the actin solution. Ratios between 1:100 and 1:1000 labeled phalloidin molecules to actin monomers were used for quantitative measurements.

All fluorescence and crossed polarization images were taken using a Nikon E800 microscope equipped with a CoolSnap HQ camera (Photometrics, Tucson, AZ). All polarization images were taken with the polarizer and analyzer oriented vertically and horizontally, respectively, unless otherwise noted in the image caption. Images were taken in the middle of the capillary cavity, well away from the glass walls of the capillary and any air-liquid interfaces.

C. Birefringence measurements

Birefringent materials have indices of refraction which depend on direction. These indices are named after the decomposed wave parts, called the ordinary (n_o) and extraordinary (n_e) waves. The birefringence of the material is then defined as $\Delta n = n_e - n_o$. Birefringence data were measured using the PolScope package from Cambridge Research & Instrumentation, Inc. (Woburn, MA). PolScope measures the optical birefringence and the slow axis direction for each pixel, therefore giving a measure of the local alignment [43,44]. Birefringence data are reported as a specific retardance $\Delta d/c$, which is related to the optical birefringence as $\Delta d = \Delta n\, d$, where d is the sample thickness and c is the concentration. All data were measured on the same Nikon microscope used for the fluorescence and polarization imaging.

D. Tactoid shape analysis

Following the shape characterization first introduced by Zocher and Török [45] and established in the literature [35,38], the tactoids were analyzed by measuring the long and short axes, as illustrated in Fig. 1(a). From these measurements two parameters used to define the tactoids are calculated using the equations

$$R = \frac{r_1^2 + r_2^2}{2r_2}, \tag{1}$$

$$\alpha = \arccos\left(1 - \frac{2r_2^2}{r_1^2 + r_2^2}\right). \tag{2}$$

Figure 1(b) shows representative examples of this characterization applied to a few tactoids of F-actin. It is clearly seen that this description accurately depicts each tactoid, maintaining the two sharp points along the long axis and fully capturing the shape.

Two different and independent treatments have modeled and analyzed the tactoid shape and shown how it results

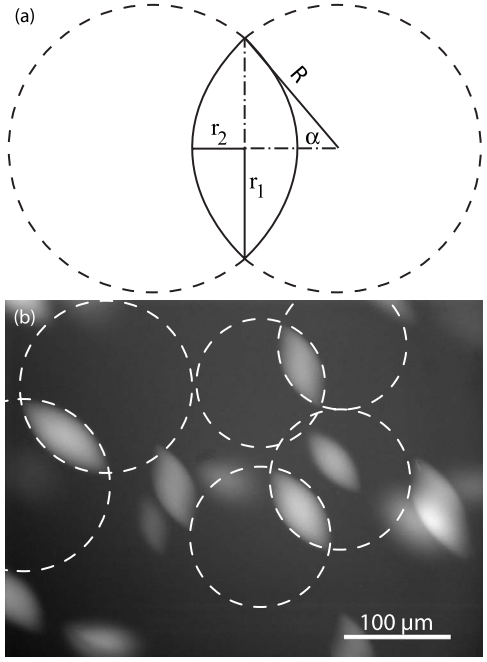

FIG. 1. (a) A tactoid is defined by the following related parameters: (r_1, r_2) or (R, α). The tactoid is considered to be the volume created by rotating the region of two overlapping circles. The major and minor axes of the overlapping region are defined as r_1 and r_2, respectively. The radius of the overlapping circles is given as R, while α represents the angle corresponding to half the arclength of the overlapping region. The relations between these parameters are given in Eqs. (1) and (2). (b) A group of tactoids are shown with their defining circles. The overlapping regions are seen to clearly bound the tactoids, suggesting that this characterization accurately captures the defining features of the tactoid.

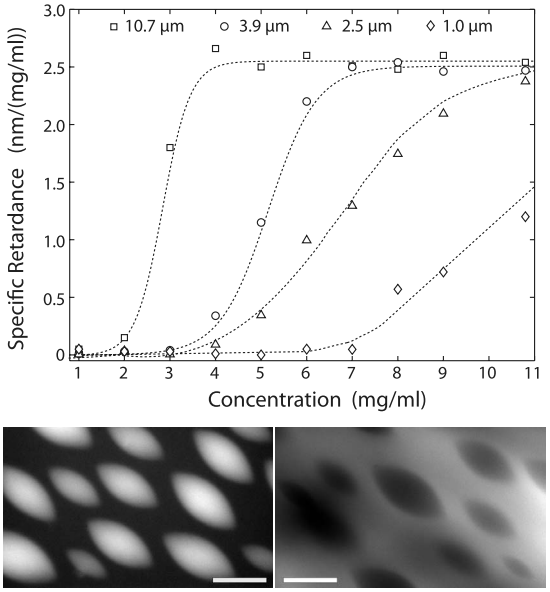

FIG. 2. The specific retardance of F-actin is plotted as a function of concentration with varying average filament lengths. F-actin solutions with average filament lengths of 10.7 μm (□), 3.9 μm (○), 2.5 μm (△), and 1.0 μm (◇) are shown. The dashed lines are guides for the eye. Tactoids are only seen for solutions along the curve farthest to the right. Shown below the plot are two representative images of tactoid formation: nematic tactoids in an isotropic background (bottom left) and isotropic tactoids in a nematic background, sometimes referred to as atactoids [29] (bottom right). Scale bars are 50 μm.

from a minimization of the free energy. Prinsen and van der Schoot [35–37] use the parameters r_1 and r_2, while Kaznacheev *et al.* [38,39] use R and α. These treatments are computationally intensive and are based upon a number of idealizations to simplify the simulations. For our system these idealizations almost certainly do not hold, making it difficult to apply the theories directly. The application of either theory is further compromised by the fact that our system is dynamic, consisting of a spread of filament lengths and filaments which are constantly changing due to treadmilling. Nevertheless, these theories are still useful in understanding the basic structure of the tactoids and identifying trends in the data. As such, we have given a brief review of one of the less computationally intensive analyses in the Appendix and have used the resulting formulas to provide a fit to our data. We recognize that the fit is not ideal, but it highlights our conclusion that the trends predicted by both methods are exhibited and consistent with our system.

III. RESULTS AND DISCUSSIONS

It is only recently that the right combination of conditions has been found for direct observation of a first-order phase transition in solutions of F-actin [28]. Coexistence and domain separation, characteristics of a first-order phase transition, require both high concentrations and short average filament lengths. Figure 2 illustrates the connection between these two parameters. The two plateau values of the specific retardance, a measure of alignment [16], indicate the isotropic and nematic regions. The transition region lies between these two plateau values. The concentration range of the isotropic to nematic transition increases as the average filament length decreases. For samples with an average filament length ≤ 2 μm, it is just past the onset of this transition where we routinely find tactoidal droplets of aligned F-actin filaments. These droplets can be treated as domains of the nematic liquid-crystalline phase.

The tactoids are distinctive in shape with two pointy ends, termed boojums [35–37]. Seen under crossed polarizers, they sometimes exhibited dark regions that made them appear asymmetric. This apparent asymmetry is shown in Fig. 3(a) to be a result of the alignment of the filaments within the tactoid with respect to the polarization axes. The director field in the nematic tactoids appears to be bipolar, continually tangent to the surface and ultimately converging at each boojum. A tactoid with such a bipolar director field overlaid is shown in Fig. 3(b). It can be seen that the dark regions in the nematic tactoid correspond to an alignment parallel to one of the polarizers (shown in the upper right corner). The brightest regions are those with an alignment of 45° with respect to the polarizers, again as expected. It is important to bear in mind, however, that most filaments are not perfectly aligned. The director field is merely the average alignment in the region. In reality, filaments will deviate slightly from the

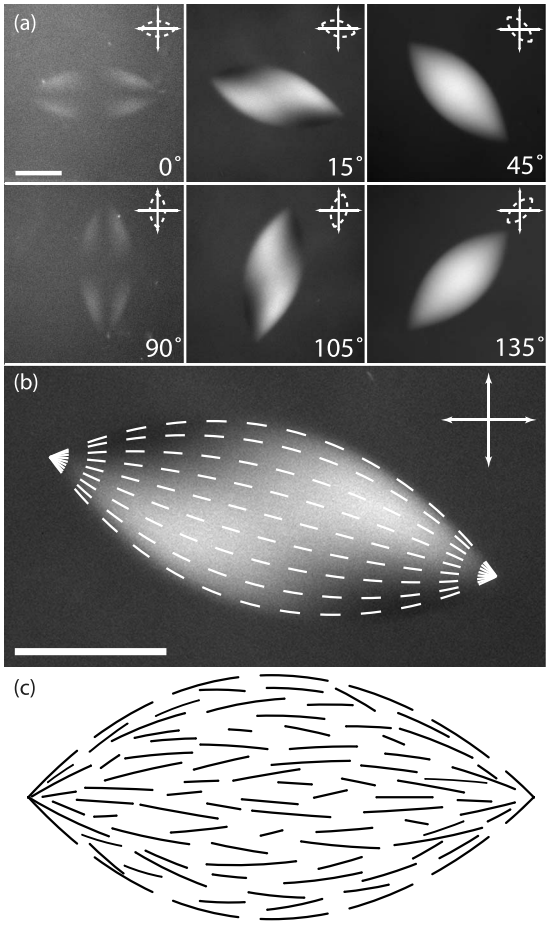

FIG. 3. Different orientations of the director field under crossed polarizers leads to an optical effect that makes the tactoids appear asymmetric. Scale bars are 25 μm. (a) A tactoid is shown rotated through various angles. The inset in each frame shows the tactoid in relation to the polarizers. The brightest regions correspond to an average alignment 45° from the polarizers. Dark regions represent an average alignment along either polarizer or regions with no average alignment. The dark regions in the tactoid are shown to migrate as the tactoid is rotated with respect to the polarizers, corresponding always with the regions where the director field is aligned along one of the polarizers. This also confirms that the director field is bipolar. (b) The tactoid at 15° is enlarged and overlaid with a bipolar director field. (c) A diagram representing the filaments inside of a nematic tactoid. Individual filaments are not perfectly aligned, but the average direction corresponds to a field as shown in (b). The diagram is not drawn to scale. The actual filaments are shorter and thinner, in addition to being many times more numerous than depicted.

path of the director field as shown in Fig. 3(c). The average alignment is quantitatively defined as the orientational order parameter, which has recently been measured to be approximately 0.75 for the F-actin nematic phase [7].

The finding of a bipolar director field sheds more light upon the free energy minimization of the actin system. Both theoretical treatments mentioned above have shown that the boojums are in fact virtual [36,39]. This is to say that they do not actually reside on the drop itself, but rather somewhere outside the drop's volume, though still on the tactoid's long

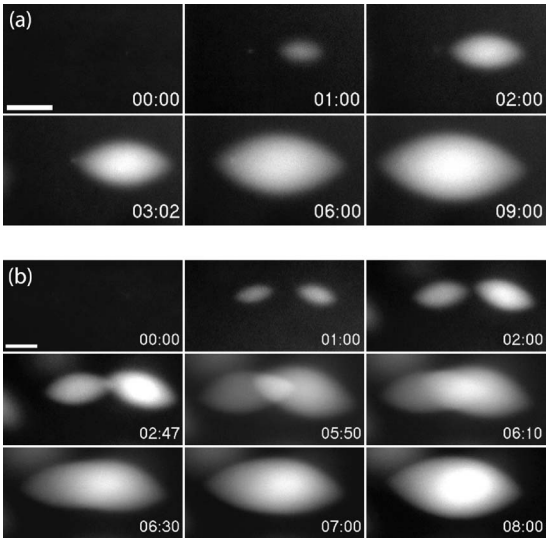

FIG. 4. Tactoids are shown to grow through a process of nucleation, growth, and coalescence in a 10.8 mg/ml solution with an average filament length of 1.3 μm. The scale bars are 25 μm and the time format is given in h:min. (a) A nematic tactoid grows in isolation over a period of 9 h. (b) During the growth process neighboring tactoids can be seen to coalesce into a single tactoid. The resulting product retains the familiar shape and characteristics of a tactoid. It is interesting to note that the process of coalescence does not seem to impact either the rate of growth or the final size of the tactoid.

axis. The distance of the virtual boojum from the physical pointed end of the actual drop is determined by the curvature of the director field. A virtual boojum infinitely far from the drop corresponds to a homogenous director field, while one right near the surface corresponds to a bipolar director field. As can be seen in Fig. 3, the director field is clearly bipolar, suggesting that the virtual boojums lie just outside the tactoid surface. This would then indicate that there is a very large interfacial tension.

The vast majority of tactoids tend to form with their long axes aligned in roughly the same direction, parallel with the capillary long axis. The tactoids appear via two distinct mechanisms: nucleation and growth and spinodal decomposition. The initial concentration and the average filament length of the solution determine which mechanism predominates. Solutions just past the onset of the isotropic to nematic transition exhibit nucleation and growth. Solutions roughly in the middle of the transition region tend to exhibit spinodal decomposition.

A. Nucleation and growth

Looking at the rightmost phase transition curve in Fig. 2, nucleation is seen to occur at the point where the specific retardance just begins to increase. An example of a tactoid nucleating can be seen in Fig. 4(a). Two tactoids that nucleate in close proximity to each other often coalesce to form a single tactoid, as seen in Fig. 4(b). As the tactoids nucleate in the solution, they all tend towards approximately the same size. Interestingly, this size seems to be independent of the

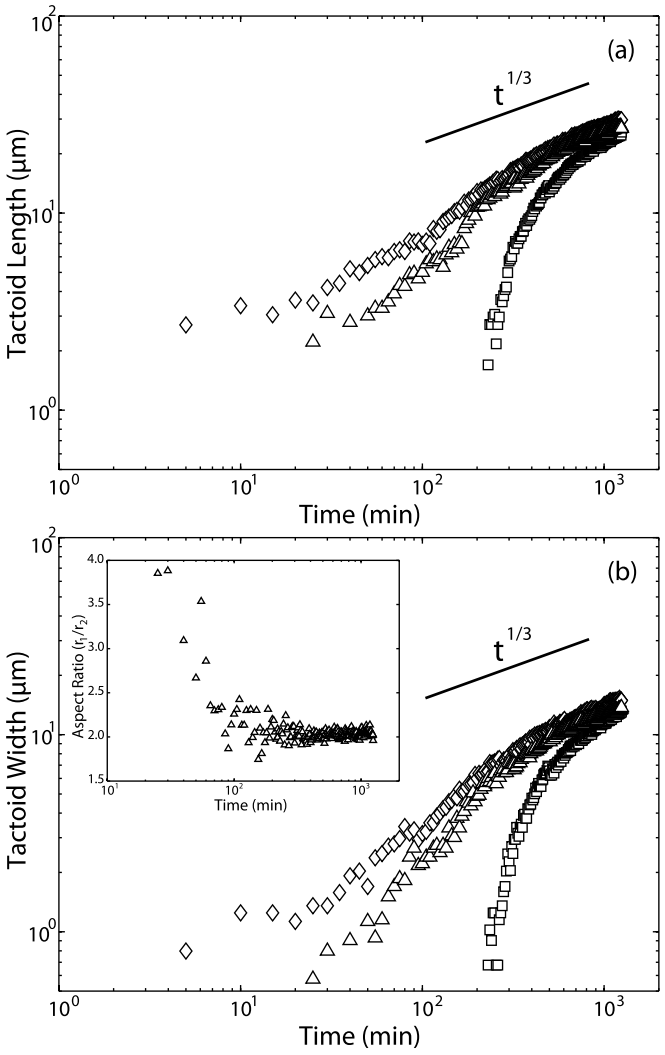

FIG. 5. The length (a) and width (b) of three nucleating tactoids were measured using time-lapse microscopy. All three tactoids reached approximately the same final size despite nucleating at different times. The tactoids that nucleated later grew much faster, until they caught up with those that nucleated earlier in the same sample. No further growth was seen after ~1200 min. The inset shows a plot of the aspect ratio with respect to time for one of the tactoids.

time when the nucleation begins. Figure 5 shows a typical example of three tactoids nucleated in a solution. Two of the tactoids began to form at roughly the same time. A third tactoid began to grow a few hours later, but all three approached the same size half a day or so after the sample was prepared. Growth ceased after ~1200 min, and no additional change was seen in the tactoid's size over the next several days (data not shown). This final size was consistent with the rest of the tactoids found in the capillary.

During the nucleation process the tactoids maintained almost a constant aspect ratio [inset in Fig. 5(b)]. It is only initially that the tactoids exhibited an extremely elongated shape. As growth continued, the tactoids filled out, settling at an aspect ratio of about 2. The tactoids maintained this constant aspect ratio until the growth finally tapered off.

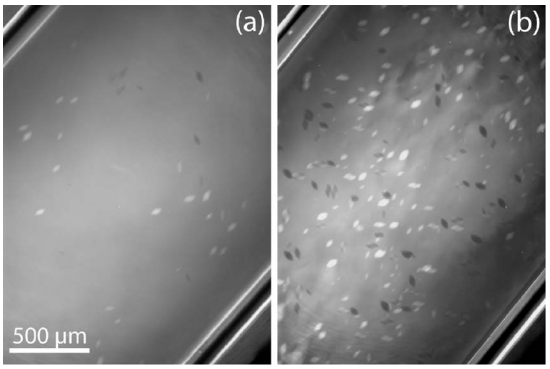

FIG. 6. A capillary seen under 4× magnification using crossed polarizers. (a) Nucleation has occurred in the capillary. There are only a few tactoids present, and all are approximately the same size. (b) The same capillary in (a) has been sonicated and allowed to relax for ~100 h. The solution is again in a steady state but now exhibits a large range of sizes, in addition to having a much greater density of tactoids.

B. Tactoid size and shape

Despite the fact that most of the tactoids grew to the same final size and no further phase separation was evidenced, the system may not have reached a unique equilibrium state following this method of preparation. Small mechanical perturbations could alter the established order. Strong shaking or sonication could completely disrupt any alignment in the capillary. After a strong perturbation the system would again settle into a steady state over time. During this perturbing process the large nematic tactoids were broken into many small uniformly distributed regions, giving the system a fine granular appearance. Examination under high magnification revealed no common shape or features. As the system relaxed, the regions coalesced into large isotropic and nematic domains. Further nucleation was rarely seen, and absent external perturbation, the system remained in this relaxed steady state indefinitely.

Perturbed systems always showed a much greater range of tactoid sizes, all retaining the familiar bipolar tactoid shape. This is in direct contrast to capillaries exhibiting nucleation and growth without additional perturbation, where all the tactoids tended towards the same approximate size. An example of this is shown in Fig. 6. Figure 6(a) shows a capillary that exhibited nucleation and growth. The capillary appears largely isotropic, and the few tactoids present are all roughly the same size. Figure 6(b) shows the same capillary ~100 h after sonication. The solution has again reached a steady state, but the number of tactoids has increased dramatically, with a wide range of different sizes.

We have chosen to use capillaries that have been perturbed and allowed to relax as samples for quantitative analysis because it seems probable that such a system is closer to equilibrium than a system exhibiting the initial nucleation seen immediately after injection. The reasoning behind this is best discussed through the context of metastability and is addressed in Sec. III D of this report. To ensure that the system is indeed in a steady state, the capillaries have been allowed to settle for a period of days after the

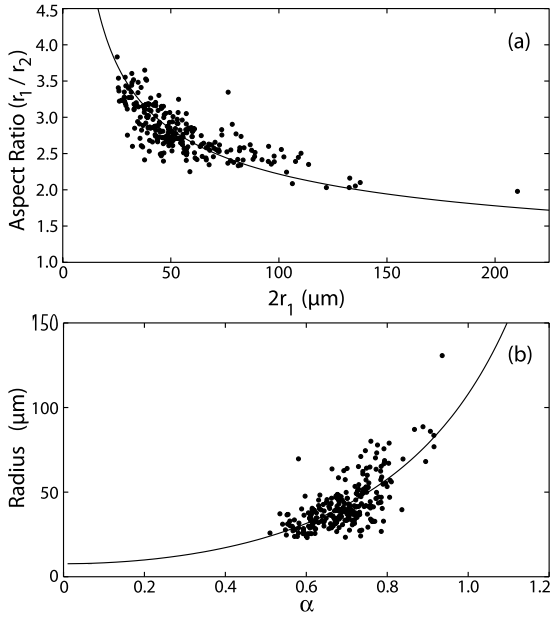

FIG. 7. Nematic tactoids in an isotropic background were measured in a capillary that was shaken and allowed to settle. The sample contained a 10.8 mg/ml actin solution with $\ell=1.2$ μm. (a) Following the convention of [35,36] the graph shows the tactoid aspect ratio plotted against the length of their long axis. The solid line is identical to the fit discussed in (b), but plotted in terms of aspect ratio against long axis. (b) The same data from above is converted to the convention of [38,39] using Eqs. (1) and (2) and plotted along with a solid line fitted using Eq. (A6), which is explained in the Appendix. The fitting parameters are $K_1/\sigma=1.92\pm0.57$ μm and $K_3/\sigma=103.4\pm8.6$ μm, where K_1 and K_3 are the splay and bending elastic constants and σ is the surface tension. The general trend of the data is consistent with the numerical work of both treatments, though an appreciable scatter in the data suggests that the tactoid's size and shape are not tightly controlled.

perturbation. Measurements were made only after the solution showed no further phase separation for an extended period of time.

A number of tactoids in one such perturbed and then fully relaxed system have been measured and plotted in Fig. 7(a) as a function of their aspect ratio against the length of their long axis and in Fig. 7(b) as a function of R versus α. The plots show the general features of the tactoid shape; solid lines in the figure represent a fit to the function given in Eq. (A6) using the formulation found in [38]. The general trend of the fit reflects that of the data: smaller tactoids tend to have significantly larger aspect ratios, and an increase in tactoid size leads to a nearly constant aspect ratio. The system exhibited a large range of variation, as evidenced by the large spread in aspect ratio and radius for any given dimension, especially for the smaller tactoids. This large variation in the measured tactoids illustrates a heterogenous structure which is again suggestive of metastability.

Following the procedure outlined in the Appendix, the two fitting parameters were found to be $K_1/\sigma=1.92\pm0.57$ μm and $K_3/\sigma=103.4\pm8.6$ μm, with $K_3/K_1=53.9$, for the data presented above. K_1 and K_3 are the splay and bending elastic constants, respectively, while σ is the surface tension at the interface of the coexisting isotropic and nematic domains. The value of σ is not known, but may be estimated once the elastic constants of the system are measured. These values are representative of several data sets taken. The magnitude of the K_3/K_1 ratio found, however, is well above that observed in many traditional liquid crystals [21], including polymer liquid crystals such as PBG [46] and the tobacco mosaic virus (TMV) [47], although it does agree with the value found by Kaznacheev *et al.* for vanadium pentoxide [38]. A large value of K_3/K_1 indicates a large bending elastic constant, which is consistent with the approximation of the actin filaments as semiflexible hard rods. This large ratio also implies a comparatively small splay elastic constant. One intuitive explanation of the small splay constant may lie in the polydispersity of the F-actin system. Short filaments can more readily fill the uneven local spacing caused by splay. A large bending elastic constant, given that the tactoid is bipolar, also implies a strong anchoring, or high anisotropy of the interfacial tension [36], which is again consistent with the director fields seen in the actin tactoids. The prolate shape of the tactoids also seems physically reasonable given the high energy price of bending compared to splaying.

C. Spinodal decomposition

An entirely different situation was seen for solutions that were approximately halfway between the isotropic and nematic phases following the rightmost curve in Fig. 2. Solutions in that part of the phase diagram underwent the process of spinodal decomposition as illustrated in Fig. 8. Directly after the preparation, the solution was temporarily aligned due to injection into the capillary. Almost immediately, the solution started to separate into nematic and isotropic regions. Under higher magnifications it was clearly evident that the nematic and isotropic pockets showed little of the distinctive tactoid characteristics seen earlier in samples exhibiting nucleation and growth. Instead the solution took on the appearance of two immiscible liquids. After this quick dissociation into nematic and isotropic pockets, the separation seemed to slow down as the process continued over several hours, finally settling into larger isotropic and nematic domains. Tactoids were almost always present in this final settled sample.

Spinodal decomposition is a phenomenon of rapid phase separation that is known to occur in binary fluids and other mixtures and recently has been seen in polymer mixtures [48]. Phase separation by spinodal decomposition can be understood as a result of negative curvature in the free energy diagram [49,50]. All solutions undergo random thermal fluctuations, but if the curvature of the free energy diagram is negative, these random fluctuations actually decrease the free energy. The fluctuations therefore become amplified over time, ultimately leading to phase separation in the system. This process has been seen in a number of systems similar to F-actin, including polymer solutions and gels [51], hard rods [52], rodlike micelles [53], and viruses [54]. A number of theoretical works also predict this behavior [55,56]. Our observations of F-actin polymerized in capillaries are consistent with all these clear characteristics of this mode of phase separation.

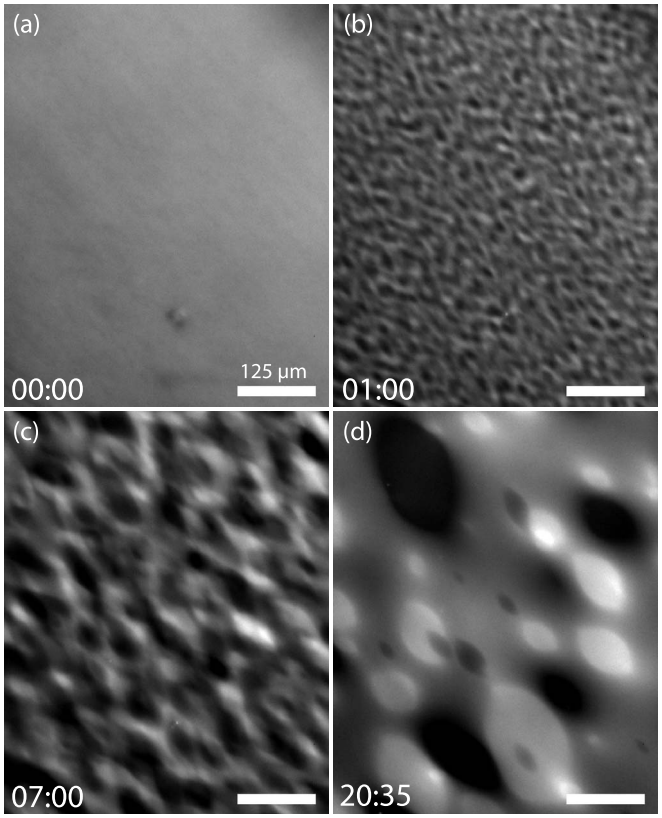

FIG. 8. A solution of 10.8 mg/ml F-actin with an average filament length of 1.4 μm underwent the process of spinodal decomposition. The images were captured using crossed polarizers oriented horizontally and vertically under 4× magnification, and the time format is given as h:min. (a) The initial state of the solution showed almost uniform alignment within the capillary. This alignment was a residual effect of injecting the solution into the capillary directly after polymerization. (b) Almost immediately (within minutes) the solution began to show a breakdown in the initial alignment. What looked like small pockets of isotropic and nematic domains appeared. (c) After 7 h the solution showed larger isotropic and nematic regions, though none showed the distinctive tactoid shape. The kinetics at this point slowed down considerably, showing very little change over a few hours. (d) Finally after almost a full day, the solution settled into a metastable state with both isotropic and nematic tactoids present in a weakly aligned nematic background.

In an effort to compare the growth of the nematic regions by spinodal decomposition to the nucleating tactoids, we developed a method of characterizing the domain size of regions undergoing spinodal decomposition. We first applied a two-dimensional fast Fourier transform (FFT) to the stack of images which revealed a clearly anisotropic pattern, as shown in Figs. 9(a) and 9(b). Defining the width of the spinodal domains as the direction along the long axis of the transform and the length as that direction perpendicular to the width, we calculated the average radial intensity of the transform. Specifically, the radial intensity was found by averaging the value within a small wedge, one oriented in each direction. This provided enough data points to get an accurate average value. When plotting these average radial intensities as a function of distance from the center of the transform, the data were fitted to a polynomial function, further reducing the amount of noise. Plots of these fits show a clearly progressing peak over time, shown in Figs. 9(c) and 9(d). We then marked the position of this peak as the characteristic measurement of domain size at each time step. The entire series of points is shown in Fig. 9(e). The final size of the domains is roughly the same order of magnitude as the tactoids that nucleate, as seen in Fig. 4.

As a simple approximation we assume that the fluctuations in density are periodic in the beginning stage of the spinodal decomposition—i.e., $C(x)=C\sin(2\pi x/\lambda)$, where C represents the amplitude of the wave. The wavelength of this periodic approximation corresponds to the onset peak value at the beginning of Fig. 9(e). This periodic function then describes the transition from isotropic to nematic domains, the maximum slope of which is given by $2\pi C/\lambda$. Assuming the difference in concentration between an isotropic and a nematic domain to be $2C$, and dividing this difference by the maximum slope, we can estimate an upper bound for the thickness of the interfacial region. Using this estimate gives the following relation between the interfacial thickness Δ and the wavelength:

$$\Delta \approx \lambda/\pi. \tag{3}$$

This estimate is in general agreement with the approximation given by Bates and Wiltzius [57], differing by only a factor of 2. Using the peak wavelength as measured for the early constant width of the tactoid in Fig. 9(e), we find the upper bound of the interfacial thickness to be roughly 3.6 μm for this spinodal system. In the future and with better techniques, it may be possible to further quantify the dimensions of this interface between the isotropic and nematic domains.

Looking further at the characteristic wavelength that was measured, the change in wavelength can be compared to the growth rate laws developed for spinodal solutions [49,50]. The average domain size a is expected to be constant in the initial stages and then transition to a growth rate of $\sim t^{1/3}$ as diffusion slows and coarsening occurs. Solid lines in Fig. 9(e) indicate these two regimes. The data are consistent with these growth rate laws, although the practically useful observation time spreads less than two orders of magnitude. It should also be mentioned that the rate law for nucleation and growth is similarly $t^{1/3}$ [58]. We believe, nonetheless, based upon the visual evidence and the clearly evolving peak in the inverse wavelength seen in the FFT, that this system is undergoing spinodal decomposition, at least during the early stage of phase separation.

D. Metastability

Earlier analysis of this system suggests that a steady state of an F-actin sample showing isotropic and nematic coexistence may not be in equilibrium, but is instead only metastable. The most obvious indication of this is that even small perturbations alter the system, and once altered, the system never returns to its previous state. This would imply that there are a number of steady states, none of which are strongly preferred above the others. A dramatic example of this is seen in Fig. 6. During their original nucleation all the

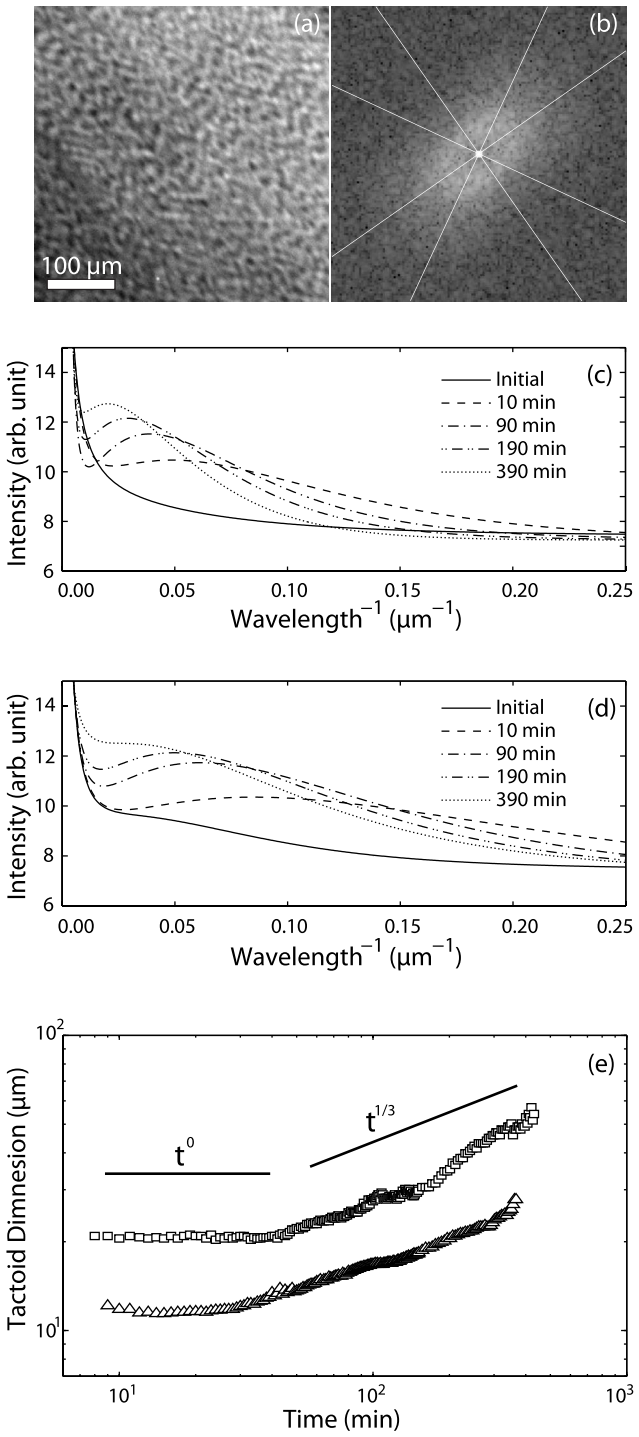

FIG. 9. The characteristic length and width of the spinodal regions were determined by taking an image (a) and performing a two-dimensional fast Fourier transform (b). The transform is clearly elongated at an angle of roughly 50° from the horizontal. The average intensity was calculated as a function of distance from the center of the transform within a 30° wedge directed along the two major directions. Fits to plots of these average radial intensities show a peak that gradually shifts towards the center of the transform for the length (c) and width (d). The length (□) and width (△) wave vectors were determined by the position of this peak. The peak is seen to steadily progress towards the origin, indicating an increasing domain size (e).

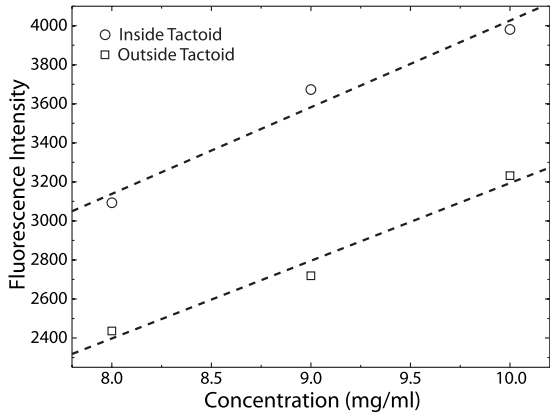

FIG. 10. Tactoids were prepared in a thin (100-μm) capillary and allowed to grow until they were flattened by the capillary walls. Intensity measurements were recorded for the regions completely filling the capillary space between both walls. Regions well beyond the domain of the tactoid were averaged to calculate the intensity value outside of the tactoid. Each data point represents an average of a number of tactoids. For a true first-order transition we would expect the average intensity to remain constant in both regions. The roughly linear increase shows that the actin concentration of both coexisting domains increase with the average concentration of the initially uniform solution of actin. This result strongly suggests that the system is only in a metastable state.

tactoids tend to be similar in size, but in the perturbed system they show a wide variety of sizes and aspect ratios. This variety can also be seen in Fig. 7, with the large spread in the data.

One plausible explanation for this phenomenon is that there exists an energy barrier which prohibits the onset of nucleation. This barrier keeps the solution in a uniform state at concentrations beyond those where one would expect phase separation. Once the barrier is overcome, however, it becomes energetically favorable to recruit neighboring filaments, with regions growing in size and increasing the local alignment, ultimately creating two separate phases. Because of this nucleation barrier, solutions on the cusp of the transition region show only a small number of tactoids and occasionally a weakly aligned background. The process of perturbation can then be thought of as breaking up the existing tactoids into a number of small seeds which are distributed throughout the capillary. These seeds, having already overcome the initial nucleation barrier, provide a number of nuclei for the nematic droplets to grow around. This prevalence of nuclei results in a large number of tactoids forming in the capillary. The wider range of sizes of tactoids could then be attributed to the coalescence of neighboring seeds in a stochastic fashion. Local areas in the capillary with a high concentration of these seeds would form larger tactoids. Areas with only a few seeds would end up with smaller tactoids due to a lack of coalescence in their growth history.

Figure 10 shows further indications of metastability. The plot shows the average value of the fluorescence intensity both inside the tactoids and outside in the surrounding isotropic solution. The fluorescence intensity is directly related to the concentration of actin. Thin capillaries, 100 μm thick, were filled with solutions of F-actin. The tactoids grew large

enough to be flattened by the top and bottom walls of the capillary. The average fluorescence intensity was then measured only in this region where the nematic solution filled the entire depth of the capillary. For a first-order phase transition, one would anticipate the actin concentration within each coexisting phase to remain unchanged as the average solution concentration is increased. The volume fraction of the solution found in the nematic phase would be expected to increase, but since the concentrations of the phases remain constant, the average fluorescence intensity within each phase should be unaltered. Here, instead, a rise is seen in the fluorescence intensity of both the isotropic and nematic regions as the average concentration of the solution increases.

A third indicator of metastability is seen in the fact that isotropic and nematic tactoids are often found in a weakly aligned background, as indicated in Fig. 8(d). In a true first-order transition we would not expect the background to show any alignment. This feature is seen in almost all the spinodal decomposition movies that have been recorded and is found also in perturbed samples that have been allowed to relax. The phenomenon of solutions having a weakly aligned background is not limited to F-actin. Other biopolymers such as DNA [59,60] and Pf1 bacteriophage [61] also exhibit this type of behavior, which have been described as precholesteric or paranematic. One common characteristic of these systems is that the biopolymers are large and perhaps entangled even when in the aligned phase. Thus they would be prone to exist in metastable states that could be stabilized by very weak additional interactions.

As the filaments are charged, it is also likely that there is some electrostatic interaction between them and the glass surface, which tends to hold a net negative charge. To avoid this additional complication, all tactoids measured were those in the center of the capillary, far from the glass surface. Nematic regions found at the glass surface of the capillaries often showed a deformed tactoid shape, but were not included in the analyses described above. This additional effect may, in part, be responsible for the metastability of F-actin and other similar systems.

IV. SUMMARY AND CONCLUSIONS

We have shown that solutions of F-actin do indeed undergo a first-order transition from the isotropic to nematic state. This transition is highly dependent upon the average filament length of the F-actin and also on the protein concentration. At high concentrations and short average filament lengths, the solution phase separates into nematic droplets in an isotropic background. These tactoids display the same characteristics as other rodlike polymer systems that have been studied. It has been suggested that the shape of the tactoids is the result of a minimization of the free energy. By applying such a treatment to a solution with tactoids in a steady state, we find that the general trend of the data does indeed follow theoretical predictions.

The tactoids have been shown to form through two methods: nucleation and growth and spinodal decomposition. Both processes result in the formation of tactoids and provide further evidence of a first-order phase transition. The domain size in each of the two growth regimes are of the same order of magnitude and occur over similar spans of time. The F-actin system also displays many characteristics of metastability. Additional characteristics not accounted for in this basic liquid-crystal treatment, including a nucleation energy barrier, interactions between filaments, polydispersity, and the dynamic nature of F-actin, all likely play a role in rendering F-actin solutions metastable.

ACKNOWLEDGMENTS

We would like to thank Peter Prinsen and Professors Paul van der Schoot and Patrick Davidson for helpful communications. We would also like to thank Professors Robert Meyer and Thomas Powers for their helpful suggestions. This work has been supported by the National Science Foundation (NSF) awards DMR 0405156 and DMR 0079964 (MRSEC), and the Petroleum Research Fund (PRF 42835-AC7), administered by the American Chemical Society.

APPENDIX

Presented below is a brief outline of the analysis by Kaznacheev *et al.* [38], used in fitting the data from our measurements (Fig. 7). Readers interested in the details of the derivation are referred to the original paper.

The tactoids are modeled as three-dimensional droplets, each created by revolving the overlapping region of two circles about its long axis. From the images taken with the microscope the tactoid's long axis r_1 and short axis r_2 are measured. Using Eqs. (1) and (2) these are then related to the radius R and angle α of the defining circles shown in Fig. 1(a).

There are two sources of energy that must be considered when discussing the tactoids. One is the elastic energy of the rodlike suspension and the other is the interfacial tension between the two phases. The elastic free energy of a liquid crystal is given by

$$F_E = \int_V d^3\mathbf{r}\left[\frac{1}{2}K_1(\boldsymbol{\nabla}\cdot\mathbf{n})^2 + \frac{1}{2}K_3[\mathbf{n}\times(\boldsymbol{\nabla}\times\mathbf{n})]^2\right], \tag{A1}$$

where K_1 and K_3 are the splay and bending elastic constants. This expression ignores a term containing K_2, the twisting elastic constant, which is assumed to contribute negligibly to the free energy. The interfacial energy is given by

$$F_S = \sigma S, \tag{A2}$$

where σ is the surface tension and S is the surface area of the tactoid. Given the geometric representation of the tactoid discussed earlier, the surface contribution to the free energy can be calculated as follows:

$$F_S = 4\pi\sigma R^2(\sin\alpha - \alpha\cos\alpha) \tag{A3}$$

Furthermore, if a constant volume is assumed for the tactoidal drop, a relationship can be derived between R and α,

$$V = 2\pi R^3\left(\sin\alpha - \alpha\cos\alpha - \frac{\sin^3\alpha}{3}\right). \tag{A4}$$

Calculating the two elastic terms is not as straightforward as the surface term. If the director field of the nematic drop is defined as tangent to the surface of the drop [Fig. 3(b)], it is found that

$$F_E = 4\pi RK_1(\sin\alpha - \alpha\cos\alpha) + \pi RK_3(3\sin\alpha - 3\,\alpha\cos\alpha - \alpha^2\sin\alpha). \tag{A5}$$

Finally, putting all this together and dividing through by $\sigma V^{2/3}$, a dimensionless free energy expression is found. Minimizing this result with respect to α and solving for R yields the following expression:

$$R = \frac{K_1}{\sigma}f_1(\alpha) + \frac{K_3}{\sigma}f_3(\alpha), \tag{A6}$$

where

$$f_1(\alpha) = \frac{\alpha\sin\alpha - 2\alpha^2\cos\alpha + \sin^2\alpha\cos\alpha}{\cos\alpha\,[\alpha(\alpha + \sin\alpha\cos\alpha) - 2\sin^2\alpha]} \tag{A7}$$

and

$$f_3(\alpha) = \frac{(\alpha^2 - \sin^2\alpha)[\alpha(1 + 2\cos^2\alpha) - 3\sin\alpha\cos\alpha]}{4\sin\alpha\cos\alpha\,[\alpha(\alpha + \sin\alpha\cos\alpha) - 2\sin^2\alpha]} \tag{A8}$$

This is the functional form used to fit to the data in Fig. 7(b). The two fitting parameters we find for the data shown are $K_1/\sigma = 1.92 \pm 0.57$ μm and $K_3/\sigma = 103.4 \pm 8.6$ μm. For presentation purposes Eqs. (1) and (2) have been used to translate the results of the fit back in terms of r_1 and r_2 for the plot shown in Fig. 7(a).

[1] A. R. Bausch and K. Kroy, Nat. Phys. **2**, 231 (2006).
[2] K. C. Holmes, D. Popp, W. Gebhard, and W. Kabsch, Nature (London) **347**, 44 (1990).
[3] T. J. Mitchison and L. P. Cramer, Cell **84**, 371 (1996).
[4] F. Oosawa and S. Asakura, *Thermodynamics of the Polymerization of Protein* (Academic Press, New York, 1975) (see pp. 34–35).
[5] E. D. Korn, M.-F. Carlier, and D. Pantaloni, Science **238**, 638 (1987).
[6] I. Fujiwara, S. Takahashi, H. Tadakuma, T. Funatsu, and S. Ishiwata, Nat. Cell Biol. **4**, 666 (2002).
[7] J. Viamontes, S. Narayanan, A. R. Sandy, and J. X. Tang, Phys. Rev. E **73**, 061901 (2006).
[8] D. Sept, J. Xu, T. D. Pollard, and J. A. McCammon, Biophys. J. **77**, 2911 (1999).
[9] H. Isambert, P. Vernier, A. C. Maggs, A. Fattoum, R. Kassab, D. Pantaloni, and M.-F. Carlier, J. Biol. Chem. **270**, 11437 (1995).
[10] F. Gittes, B. Mickey, J. Nettleton, and J. Howard, J. Biol. Chem. **120**, 923 (1993).
[11] M. L. Gardel, M. T. Valentine, J. C. Crocker, A. R. Bausch, and D. A. Weitz, Phys. Rev. Lett. **91**, 158302 (2003).
[12] H. Isambert and A. C. Maggs, Macromolecules **29**, 1036 (1996).
[13] J. Xu, A. Palmer, and D. Wirtz, Macromolecules **31**, 6486 (1998).
[14] R. Furukawa, R. Kundra, and M. Fechheimer, Biochemistry **32**, 12346 (1993).
[15] C. Coppin and P. Leavis, Biophys. J. **63**, 794 (1992).
[16] J. Viamontes and J. X. Tang, Phys. Rev. E **67**, 040701(R) (2003).
[17] J. X. Tang and P. A. Janmey, J. Biol. Chem. **271**, 8556 (1996).
[18] J. X. Tang, H. Kang, and J. Jia, Langmuir **21**, 2789 (2005).
[19] O. Pelletier, E. Pokidysheva, L. S. Hirst, N. Bouxsein, Y. Li, and C. R. Safinya, Phys. Rev. Lett. **91**, 148102 (2003).
[20] R. Furukawa and M. Fechheimer, Int. Rev. Cytol. **175**, 29 (1997).
[21] P. G. de Gennes and J. Prost, *The Physics and Liquid Crystals*, 2nd ed. (Oxford Science, New York, 1993).
[22] A. Suzuki, T. Maeda, and T. Ito, Biophys. J. **59**, 25 (1991).
[23] L. Onsager, Ann. N.Y. Acad. Sci. **51**, 627 (1949).
[24] P. J. Flory, *Statistical Mechanics of Chain Molecules* (Interscience, New York, 1969).
[25] A. R. Khokhlov and A. N. Semenov, Physica A **108**, 546 (1981).
[26] A. R. Khokhlov and A. N. Semenov, Physica A **112**, 605 (1982).
[27] E. Helfer, P. Panine, M.-F. Carlier, and P. Davidson, Biophys. J. **89**, 543 (2005).
[28] J. Viamontes, P. W. Oakes, and J. X. Tang, Phys. Rev. Lett. **97**, 118103 (2006).
[29] H. Zocher, Z. Anorg. Allg. Chem. **147**, 91 (1925).
[30] H. Zocher and K. Jakobsohn, Kolloid. Beih. **28**, 167 (1929).
[31] P. A. Buining and H. N. W. Lekkerkerker, J. Phys. Chem. **97**, 11510 (1993).
[32] E. Barry, Z. Hensel, Z. Dogic, M. Shribak, and R. Oldenbourg, Phys. Rev. Lett. **96**, 018305 (2006).
[33] P. E. Lammert, D. S. Rokhsar, and J. Toner, Phys. Rev. Lett. **70**, 1650 (1993).
[34] P. E. Lammert, D. S. Rokhsar, and J. Toner, Phys. Rev. E **52**, 1778 (1995).
[35] P. Prinsen and P. van der Schoot, Phys. Rev. E **68**, 021701 (2003).
[36] P. Prinsen and P. van der Schoot, Eur. Phys. J. E **13**, 35 (2004).
[37] P. Prinsen and P. van der Schoot, J. Phys.: Condens. Matter **16**, 8835 (2004).
[38] A. V. Kaznacheev, M. M. Bogdanov, and S. A. Taraskin, J. Exp. Theor. Phys. **95**, 57 (2002).
[39] A. V. Kaznacheev, M. M. Bogdanov, and A. S. Sonin, J. Exp. Theor. Phys. **97**, 1159 (2003).
[40] J. D. Pardee and J. A. Spudich, Methods Cell Biol. **24**, 271 (1982).

[41] P. A. Janmey, J. Peetermans, K. S. Zaner, T. P. Stossel, and T. Tanaka, J. Biol. Chem. **261**, 8357 (1986).
[42] P. Sampath and T. D. Pollard, Biochemistry **30**, 1973 (1991).
[43] R. Oldenbourg and G. Mei, J. Microsc. **180**, 140 (1995).
[44] M. Shribak and R. Oldenbourg, Appl. Opt. **42**, 3009 (2003).
[45] H. Zocher and C. Török, Kolloid-Z. **170**, 140 (1960).
[46] S.-D. Lee and R. B. Meyer, Phys. Rev. Lett. **61**, 2217 (1988).
[47] J. A. N. Zasadzinski and R. B. Meyer, Phys. Rev. Lett. **56**, 636 (1986).
[48] K. Binder, in *Phase Transformations of Materials*, edited by G. Kostorz (Wiley-VCH, Weinheim, 2001), p. 409.
[49] R. G. Larson, *The Structure and Rheology of Complex Fluids* (Oxford University Press, New York, 1999).
[50] R. A. L. Jones, *Soft Condensed Matter* (Oxford University Press, New York, 2002).
[51] R. Bansil and G. Liao, Trends Polym. Sci. **5**, 146 (1997).
[52] M. P. B. van Bruggen, J. K. G. Dohnt, and H. N. W. Lekkerkerker, Macromolecules **32**, 2256 (1999).
[53] R. H. Tromp and P. van der Schoot, Phys. Rev. E **53**, 689 (1996).
[54] M. P. Lettinga, K. Kang, P. Holmqvist, A. Imhof, D. Derks, and J. K. G. Dhont, Phys. Rev. E **73**, 011412 (2006).
[55] J. W. Winters, T. Odijk, and P. van der Schoot, Phys. Rev. E **63**, 011501 (2000).
[56] S. B. Goryachev, Phys. Rev. Lett. **72**, 1850 (1994).
[57] F. S. Bates and P. Wiltzius, J. Chem. Phys. **91**, 3258 (1989).
[58] I. M. Lifshitz and V. V. Slyozov, J. Phys. Chem. Solids **19**, 35 (1961).
[59] T. E. Strzelecka, M. W. Davidson, and R. L. Rill, Nature (London) **331**, 457 (1988).
[60] K. Merchant and R. L. Rill, Macromolecules **27**, 2365 (1994).
[61] M. Zweckstetter and A. Bax, J. Biomol. NMR **20**, 365 (2001).